



## RAPID COMMUNICATION

# Nucleolin promotes tumor growth in colorectal cancer by enhancing hnRNPA1-mediated PKM2 alternative splicing

Emerging evidence indicates that metabolism reprogramming plays an important role in cancer progression. RNA-binding protein nucleolin (NCL) was reported to function as an important oncogenic factor in multiple cancer types.<sup>1</sup> However, the role and mechanism of NCL in cancer metabolism are unknown. In this study, we found that NCL directly interacted with hnRNPA1 and promoted CRC cell proliferation by enhancing aerobic glycolysis. Mechanistically, NCL bound PKM pre-mRNA and increased hnRNPA1-mediated PKM alternative splicing, resulting in increased PKM2 expression and tumor growth. A seed-mediated growth approach was used to synthesize gold nanostars (GNS), which were further modified with aptamer AS1411 (an NCL ligand), GE11 (an EGFR ligand), and nuclear localization signal to obtain functionalized nanoparticles (GNS-AS1411-GE11). GNS-AS1411-GE11 efficiently enter the nucleus of CRC cells and blocked the glycolysis-promoting effects of NCL, inhibiting the growth of CRC xenograft. Targeting NCL is a promising strategy for treating CRC.

To determine the RNA molecules mediating the association of NCL with proteins, we performed Flag-tag co-immunoprecipitation (Co-IP) and mass spectrum analyses to screen NCL-interacting proteins in HCT116 cells (Fig. 1A; Fig. S1A). The RBP hnRNPA1 was identified as an NCL-associated protein, and RNase A treatment almost totally abolished the association between NCL and hnRNPA1 (Fig. 1B). Additionally, immunofluorescence analyses revealed that NCL was mainly located in the nuclei of CRC cells and co-localized with hnRNPA1 (Fig. 1C; Fig. S1B). Exogenous Co-IP assays showed the same results in HEK293 cells (Fig. S1C, D).

Further, we performed RIP (RNA-binding protein immunoprecipitation) assays using an anti-NCL antibody to capture NCL-associated RNAs, among which PKM was identified by RT-PCR assays (Fig. 1D). To identify the region mediating the association of NCL with PKM, we constructed several deletion mutants of NCL and performed RIP assays. The results showed that the second RBD domain (466–710 aa) accounts for the binding of NCL to PKM (Fig. 1E, F). PKM produces PKM1 or PKM2 mRNA through alternative splicing, which is regulated by hnRNPA1.<sup>2</sup> Interestingly, NCL could also bind to PKM2 mRNA (Fig. 1D–F). Potential NCL-binding regions in PKM2 mRNA were predicted using catRAPID omics (<http://s.tartagialab.com/>) (Fig. S2A). We noticed a potential NCL-specific consensus sequence (GCCCG, 1143–1147 bp) in these regions. Thus, we generated a deletion mutation of PKM2 and repeated the RIP assays. The results showed that NCL failed to interact with the PKM2 mutant lacking the sequence (Fig. 1G).

PKM2 is the key rate-limiting enzyme regulating cellular glycolysis and is highly expressed in CRC.<sup>3</sup> Our data showed that NCL increases PKM2 expression, pyruvate kinase activity, and lactate production, thereby promoting CRC cell proliferation. NCL knockdown produced the opposite results (Fig. 1H; Fig. S2B–F). We further analyzed the effect of NCL on PKM alternative splicing using qRT-PCR as we previously described.<sup>4</sup> The results showed that NCL overexpression induced PKM2 increase, PKM1 reduction, glycolysis, and cell proliferation, which were blocked by hnRNPA1 silencing (Fig. S3). These results suggest that NCL promotes aerobic glycolysis and proliferation in CRC cells by regulating hnRNPA1-mediated PKM alternative splicing.

To analyze the interaction module between NCL and hnRNPA1, we constructed a Z-DOCK model. It was shown that 6 amino acids of NCL and 5 amino acids of hnRNPA1 were the key sites accounting for the association between

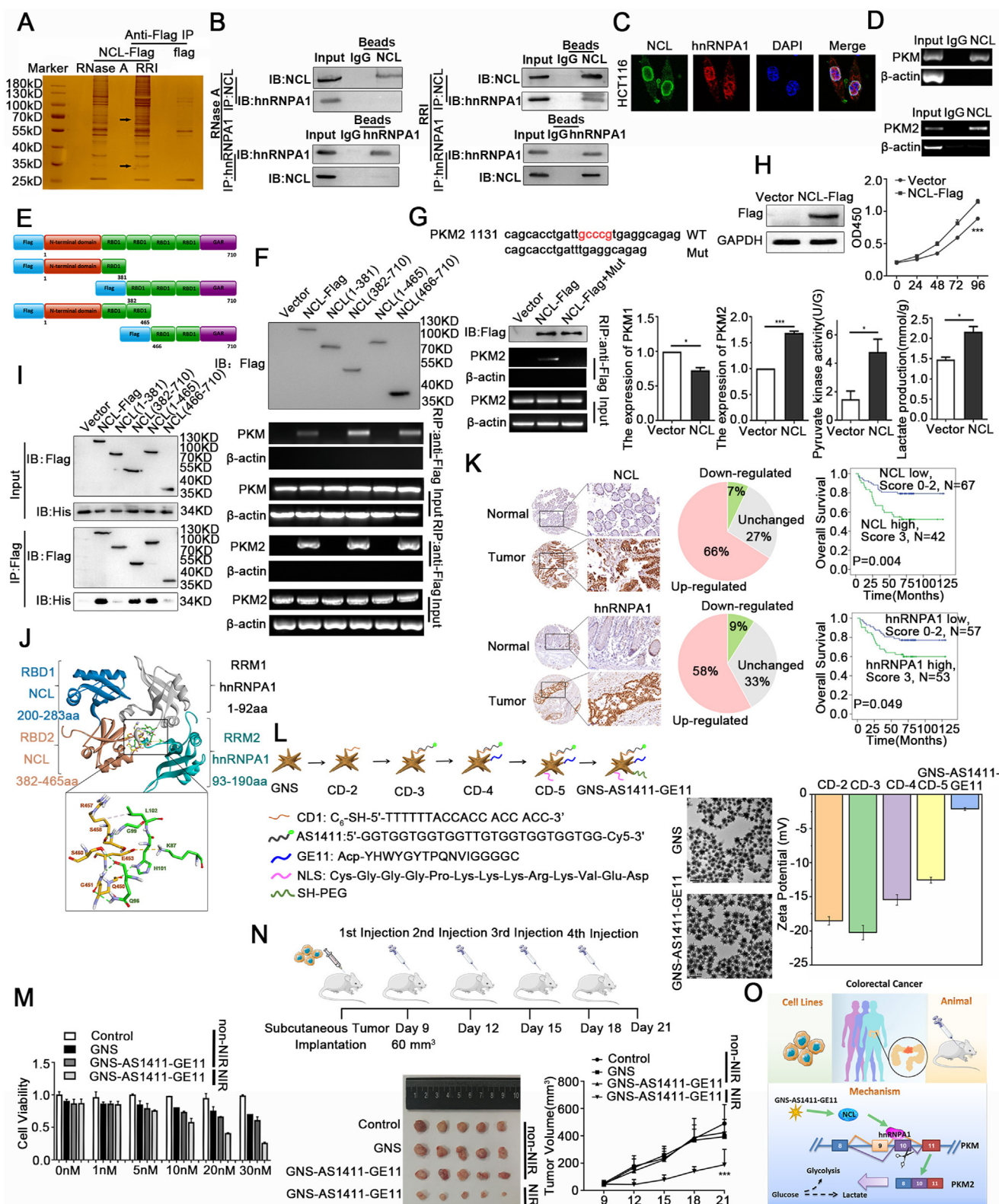


**Figure 1** NCL promotes aerobic glycolysis and tumor growth in colorectal cancer by enhancing hnRNP1-mediated PKM2 alternative splicing. **(A)** Identification of NCL-interacting proteins in the presence of RNA using mass spectrometry analyses. Lysates of HCT116 cells transfected with the NCL-Flag plasmids or the control plasmids were used to isolate NCL-interacting proteins after treatment with RNase A or recombinant RNase inhibitor (RRI), and the captured proteins were separated using SDS-PAGE electrophoresis and visualized through silver staining. **(B)** Evaluation of the association between endogenous NCL and hnRNP1 proteins in lysates of HCT116 cells treated with RNase A or RRI using Co-IP assays. **(C)** Localization of NCL and hnRNP1 in HCT116 cells by

them (Fig. 1I). We constructed several deletion mutants of NCL and performed Co-IP experiments, which showed the third RBD (382–465 aa) of NCL mediates its interaction with hnRNPA1 (Fig. 1J).

We analyzed the mRNA expression of NCL and hnRNPA1 in TCGA cohorts using the GEPIA tool (<http://gepia2.cancer-pku.cn/>). Both were higher in CRC tissues compared to normal tissues (Fig. S4A). Patients with increased NCL and hnRNPA1 mRNA expression showed a higher risk of tumor relapse (GES17537) (Fig. S4B, C), and worse overall survival rates (Fig. 1K; Fig. S4D). Moreover, NCL expression was positively correlated with hnRNPA1 levels in CRC tissues ( $R = 0.412$ ,  $P < 0.001$ ). The Cox proportional hazard analyses showed that high expression of NCL and hnRNPA1 was an independent prognostic factor for CRC (Fig. S4E). We also showed that NCL protein expression was positively correlated with the *PKM2* mRNA expression and negatively correlated with the *PKM1* mRNA expression (Fig. S4F). As we previously reported,<sup>3</sup> *PKM2* expression was associated with poor survival in CRC (Fig. S4G). These data suggest that NCL and hnRNPA1 are potential prognostic factors for CRC, and NCL positively regulates *PKM2* expression in clinical CRC tissues through hnRNPA1.

To construct an NCL-specific targeted therapy system, we designed an AS1411-conjugated nanoprobe GNS-AS1411 (Fig. 1L). However, GNS showed low efficiency to enter cells (Fig. 1L). To improve the specificity and efficiency of GNS-AS1411 in inhibiting NCL in cancer cells, GE11 and NLS were also used to modify the nanoparticle, obtaining a specific EGFR-targeting ability<sup>5</sup> (GNS-AS1411-GE11). As shown in Figure 1K, the constructed GNS-AS1411-GE11 still displayed a uniform star morphology, which was similar to the non-conjugated GNS. The average hydrodynamic diameter of GNS-AS1411-GE11 slightly increased after modifications (Fig. S5A). Furthermore, the zeta potentials also reinforced the results. After modifications, the zeta potentials of the nanoparticles were slightly reduced from  $-18$  to  $-3$  mV (Fig. 1L). Together, these data suggest the successful construction of GNS-AS1411-GE11.

We evaluated the anti-cancer activities of GNS-AS1411-GE11 in HCT116 cells which express high levels of EGFR and NCL. *In vitro* cytotoxicity assays showed that GNS-AS1411-

GE11 significantly inhibited cell viability in a dose-dependent manner, whereas non-illuminated GNS-AS1411-GE11 or GNS group only showed weak inhibitory effects at high concentrations (Fig. 1M). In addition, in HCT116 cells incubated with GNS-AS1411-GE11 (5 nM, 6 h) and irradiated with NIR, a strong fluorescence could be observed in the nuclei, suggesting that GNS-AS1411-GE11 could efficiently enter the nuclei of EGFR expressing cancer cells (Fig. S5B). Functionally, both the pyruvate kinase activities and lactate levels were significantly decreased in GNS-AS1411-GE11 treated HCT116 cells (Fig. S5C), whereas no obvious change was observed in other groups.

To further evaluate the therapeutic capability of GNS-AS1411-GE11 *in vivo*, a HCT116 xenograft mouse model was established by subcutaneous injection. Treatment with GNS-AS1411-GE11 and subsequent illumination with NIR could significantly inhibit glycolysis and tumor growth, confirming the specific therapeutic effect of the system *in vivo* (Fig. 1N; Fig. S5D–E).

In this study, we found that NCL enhances aerobic glycolysis and tumor growth by regulating hnRNPA1-mediated *PKM* alternative splicing. In addition, we designed a dual-targeting nanoparticle, which could efficiently inhibit EGFR<sup>+</sup> NCL<sup>+</sup> cancer cells, confirming NCL as a promoting target for cancer therapy (Fig. 1O).

## Author contributions

Conception and design: Z. Huang and X. Wang; Administrative support: Z. Huang and X. Wang; Provision of study materials or patients: Z. Huang, X. Wang, and H. Cheng; Collection and assembly of data: X. Wang and H. Cheng; Data analysis and interpretation: X. Wang, H. Cheng, D. Hu, Y. Chen, J. Zhao, J. Li, and W. Hassan; Manuscript writing: Z. Huang, X. Wang, and H. Cheng; Final approval of manuscript: All authors.

## Conflict of interests

The authors have no conflict of interests to declare.

immunofluorescence. (D) NCL binds to *PKM* and *PKM2* mRNA in CRC cells revealed by RIP assays. (E) The schematic diagram showed the constructed NCL deletion mutants fused with Flag-tag. (F) Identification of the domain of NCL mediating its association with *PKM* and *PKM2* mRNA using RIP assays. (G) Validation of the motif sequence mediating the binding of *PKM2* mRNA to NCL. (H) The effects of NCL overexpression on cell viability, *PKM1/2* expression, pyruvate kinase activity, and lactate production in HCT116 cells. (I) A Z-DOCK model analyzing the interaction module between NCL and hnRNPA1. (J) The third RBD of NCL (382–465 aa) mediates its interaction with hnRNPA1 revealed by Co-IP assays. (K) The protein expression of NCL and hnRNPA1 in CRC clinical samples was evaluated by IHC staining. Kaplan–Meier plots of overall survival versus NCL protein and hnRNPA1 protein. (L) The designed protocol, TEM images, and zeta potential of GNS-AS1411-GE11. (M) The effect of Nanoprobes-AS1411 on cell viability *in vitro*. (N) The effect of Nanoprobes-AS1411 *in vivo*. (O) Schematic of the underlying mechanism of NCL in promoting the tumor growth of colorectal cancer by enhancing hnRNPA1-mediated *PKM2* alternative splicing.

## Funding

This work was supported by the National Natural Science Foundation of China (No. 81802462, 81972220, and 82173063), the Natural Science Foundation of Jiangsu Province, China (No. BK20180618 and BE2019632), Wuxi Taihu Lake Talent Plan, and Wuxi Medical Key Discipline (China) (No. ZDXK2021002), China Postdoctoral Science Foundation (No. 2020M681493), Postdoctoral Science Foundation of Jiangsu Province, China (No. 2020Z050), and Fundamental Research Funds for the Central Universities (China) (No. JUSRP11952).

## Appendix A. Supplementary data

Supplementary data to this article can be found online at <https://doi.org/10.1016/j.gendis.2023.02.020>.

## References

1. Romano S, Fonseca N, Simões S, et al. Nucleolin-based targeting strategies for cancer therapy: from targeted drug delivery to cytotoxic ligands. *Drug Discov Today*. 2019;24(10):1985–2001.
2. Kuranaga Y, Sugito N, Shinohara H, et al. SRSF3, a splicer of the PKM gene, regulates cell growth and maintenance of cancer-specific energy metabolism in colon cancer cells. *Int J Mol Sci*. 2018;19(10):3012.
3. Bian Z, Zhang J, Li M, et al. LncRNA-FEZF1-AS1 promotes tumor proliferation and metastasis in colorectal cancer by regulating PKM2 signaling. *Clin Cancer Res*. 2018;24(19):4808–4819.
4. Zhao J, Li J, Hassan W, et al. Sam68 promotes aerobic glycolysis in colorectal cancer by regulating PKM2 alternative splicing. *Ann Transl Med*. 2020;8(7):459.
5. Tang H, Pan Y, Zhang Y, et al. Challenges for the application of EGFR-targeting peptide GE11 in tumor diagnosis and treatment. *J Control Release*. 2022;349:592–605.

Xue Wang <sup>a,1</sup>, Han Cheng <sup>a,b,1</sup>, Die Hu <sup>c</sup>, Ying Chen <sup>a,b</sup>,  
Waseem Hassan <sup>d</sup>, Jing Zhao <sup>a,b</sup>, Jiuming Li <sup>a,b</sup>,  
Zhaohui Huang <sup>b,\*</sup>

<sup>a</sup>Laboratory of Cancer Epigenetics, Wuxi School of Medicine, Jiangnan University, Wuxi, Jiangsu 214062, China

<sup>b</sup>Wuxi Cancer Institute, Affiliated Hospital of Jiangnan University, Wuxi, Jiangsu 214062, China

<sup>c</sup>Wuxi School of Medicine, Jiangnan University, Wuxi, Jiangsu 214062, China

<sup>d</sup>Department of Pharmacy, COMSATS University Islamabad, Lahore Campus, Lahore 54000, Pakistan

\*Corresponding author.

E-mail address: [zhaohuihuang@jiangnan.edu.cn](mailto:zhaohuihuang@jiangnan.edu.cn) (Z. Huang)

18 July 2022

Available online 27 March 2023

<sup>1</sup> These authors contributed equally to this work.